Spent Fuel Transport Associated with other Dangerous Goods in Regular Train Units -Assessment of Hypothetical Explosion Impacts-

Viktor Ballheimer, Bernhard Droste, Günter Wieser and Linan Qiao

Bundesanstalt für Materialforschung und –prüfung (BAM), Berlin, Germany

Abstract

Continental railway transport regulations (RID) do not exclude the transportation of spent fuel casks in a regular train unit that also contains wagons with other hazardous materials. In case of a train accident the release or reactions of those dangerous goods can potentially give significant accidental impacts onto the spent fuel casks. The assessment of fires from inflammable liquids and the explosion impacts from pressurized inflammable gases (like LPG) is well known from other studies which usually justified sufficient safety margins of the robust spent fuel cask designs [1].

A new problem to be assessed is the potential impact from a detonation blast wave from explosives transported in the same train unit as a spent fuel cask. BAM is assessing this problem by developing a numeric model to calculate the effect of a dynamic external shockwave pressure onto the cask construction. The calculation results show that the integrity of a robust monolithic cask with a screwed lid closure system is preserved considering the effect of a 21 t (equivalent weight of TNT) explosives detonation in the regular transport configuration with a distance of 25 m between the centre of the explosion and the cask front.

1. Introduction / Background

Analysing the problem of a spent fuel transport together with other dangerous goods it has to be considered that in Germany a wagon with the spent fuel cask has to be located behind the locomotive, and a wagon not carrying any dangerous good has to be coupled behind it. This paper presents the estimation of the resistance of the spent fuel transport cask (especially its lid system) against the detonation of explosive charges. The weight of explosives of 21 metric tons in the TNT (Tri-Nitro-Toluene) equivalence and its distance to the cask of 25 meters are conservative assumptions for hypothetical accident scenario. A monolithic, cylindrical container is considered as a reference cask. The reference cask is equipped with cylindrical, wooden impact limiters, which cover its top and bottom ends. Two examples of the screwed lid system are considered, namely the one-lid-system with elastomere gaskets of a so-called pure transport cask (T-Cask) and the double lid system with metallic gaskets in case of the transport and storage cask (TS-Cask). Only the loading by the blast wave will be discussed. The loads by fragments were not considered here. But for this, see [2] where impact loads onto a cask due to aircraft crashes was analysed.

The study presented in this paper was carried out under the assumption usually made, that the shock load can be decoupled from the structural response. First, the blast wave parameters were defined for the structure treated as a rigid body. This definition was carried out in a simplified but conservative way by comparison of various approaches proposed in the published literature. In the second step the stress and deformation behaviour of the spent fuel cask under these loads was investigated by means of the finite element (FE) analysis. For the FE calculations the program ABAQUS 6.4 [3] was used.

2. Main assumptions and explanatory notes regarding the parameters of the blast loading

The phenomenology of the explosion and the characteristics of the blast loading on the structures are investigated in a number of experimental and analytical studies (e.g. [4-8]). Before a comparison of some approaches in the published literature, we review briefly the elements of the blast phenomenon and the assumptions made here in order to define the blast loading on the spent fuel cask in a conservative way.

First it was assumed, that the explosives detonate at ground level (surface burst). The sizes of the charge and soil reaction are not taken into account and the classical point source on a rigid surface was considered.

In general, the effect of the external detonation of explosives on an aboveground structure can be described as follows:

(a) The detonation of the explosive charge W on the rigid surface leads to the sudden increase of the temperature and pressure in the centre of the explosion and finally to the hemispherical blast or shock wave moving on the ground surface outward. Fig. 1 shows schematically the ideal blast wave pulse. The shock front arrives the point R_0 at a time t_A and the incident (or side-on) overpressure in it rises abruptly to a peak value $P_{s0}(W, R_0)$. During the short time interval t_0 the incident pressure decays to ambient pressure P_0. This positive phase is followed by a negative one in which the pressure drops below the ambient value (the peak and duration are $P_{s0}^{-}(W, R_0)$ and t_0^{-}). Because of its low significance for the massive constructions under discussion here, the negative phase will be ignored.

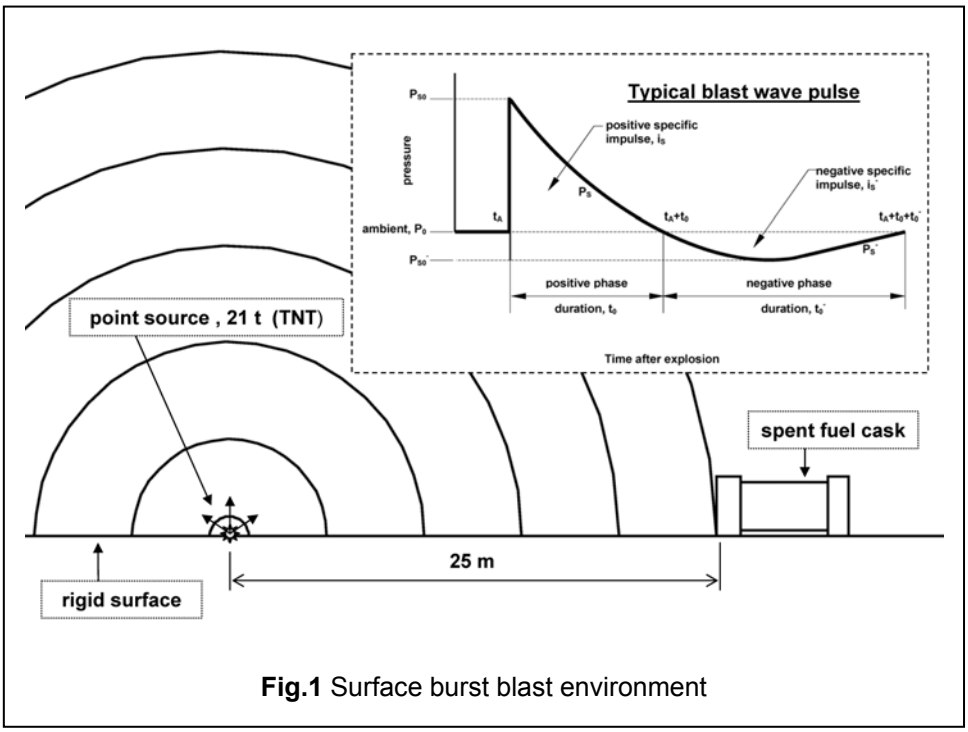

Fig.1 Surface burst blast environment

(b) If the shock wave impinges on a rigid structure with a face wall normal to the direction of wave propagation (such an orientation produces the most severe loading on the structural elements), a reflected wave travels back towards the point of explosion and a reflected pressure with a peak value $P_{r0}(W, R_0) > P_{s0}(W, R_0)$ in excess of the incident pressure is abruptly developed on the surface. At this instant the side walls and rear wall of the structure are not loaded.

(c) After the front wall is by-passed by the shock wave, the overpressure acting on it is rapidly reduced and is given by the sum of the pressure in the incident wave and the velocity impact overpressure $P_s(W, R_0, t) + k_v P_d(W, R_0, t)$ with a coefficient of sliding resistance k_v assumed to be about 0.8÷1.0. The pressure on each point of the side walls $R_0 \le R \le R_0 + L$ is given by $P_s(W, R, t)$, where L is the length of the structure in the direction of wave propagation. For the pressure on the rear wall one can write $P_s(W, R_0 + L, t) - k_r P_d(W, R_0 + L, t)$, with k_r =0.8. Of course there are the phase displacements of the inceptions of the overpressures on the different points of the structure depending on the wave front velocity.

From this schematic description one can see that the blast loads are moving pulse loads, loading different parts of the structure at different times, with varying magnitudes and durations, depending on the distance and the orientation of the structure to the centre of explosion. The exact definition of the blast loading at current instant on each point of the structure is very complicated therefore some simplifications are made additionally:

- The reference cask is considered being oriented on the rigid ground surface with its axis parallel to the direction of propagation of the shock wave.
- There are no obstacles between the centre of the explosion and the reference cask.
- The top side impact limiter protecting the lid system of the cask faces the centre of the explosion and is loaded by the reflected pressure. Its reduction due to by-passing will be ignored and the reflected pressure on an infinite rigid wall in front of the shock wave will be considered.
- The cask cylindrical wall is loaded by a uniform, axial symmetrical pressure with a peak value defined by the incident pressure at the top end of the cask. This load also acts on the surface of the bottom impact limiter.
- The loads on all surfaces of the cask are presumed to be synchronous.

The parameters of the shock wave generated in an explosion (the incident and reflected overpressures and their specific impulses, the time duration, etc.) are influenced by the distance between the blast source and the structure and the energy released by the explosion (i.e., equivalent TNT charge weight). They are defined in various manuals in form of diagrams or empirical equations normally on the basis of test results generalised by use of scaling laws. The most common form of blast scaling is Hopkinson or "cube root" scaling law in which the parameters are given as functions of a scaled distance $Z=\frac{R}{\sqrt[3]{W}}$, where R is the distance from the centre of explosion to a given location and W is the equivalent TNT mass of the explosive charge. For the problem under examination here $Z = 0.9062\, m/\sqrt[3]{kg}$ (with $R = 25\, m$ and $W = 21000\, kg$).

It is necessary to note that a number of relations for the peak incident pressure versus scaled distance has been proposed in the existing literature [4-6]. Commonly they are defined for the explosion in the unlimited atmosphere (spherical waves) but are valid for the case of explosion on the rigid surface too [4], except that $2W$ must be substituted for W, because all energy of charge W is concentrated in the hemispherical waves (we consider the ground acting as a smooth, rigid plane, which reflects all energy). Some formulae for the incident pressure in the case of surface explosion, derived from the relations defined by different authors ($Z\ in\ [m/\sqrt[3]{kg}], P_{s0}\ in\ [MPa]$) are compared in Tab. 1

Comments	incident pressure by surface explosion	Equation
Based on the numeric solution for unlimited atmosphere of an ideal gas [4, sources /18, 19/].	$P_{s0} = \begin{cases} (\frac{1.3132}{Z^3} + 0.098) & Z \le 1.14 \\ (\frac{0.1205}{Z} + \frac{0.2264}{Z^2} + \frac{1.1466}{Z^3} - 0{,}0019) & 1.14 < Z \le 12.52 \end{cases}$	(Eq.1)
Based on the theory of model similarity with the coefficient derived experimentally [4, sources /93, 114/].	$P_{s0} = \begin{cases} (\frac{2.0972}{Z^3} - 0.0980) & Z \le 1 \\ (\frac{0.0939}{Z} + \frac{0.3967}{Z^2} + \frac{1.2740}{Z^3}) & 1 < Z \le 15 \end{cases}$	(Eq.2)
Based on an experimental investigation [4].	$P_{s0} = \begin{cases} (\frac{1.7375}{Z} + \frac{0.8618}{Z^2} - \frac{0.0700}{Z^3} + \frac{0.0015}{Z^4}) & 0.05 < Z \le 0.3 \\ (\frac{0.7648}{Z} - \frac{0.0507}{Z^2} + \frac{0.4180}{Z^3}) & 0.3 < Z \le 1 \\ (\frac{0.0817}{Z} + \frac{0.6300}{Z^2} + \frac{0.6444}{Z^3}) & 1 < Z \le 10 \end{cases}$	(Eq.3)
For surface explosions [6, source /20/].	$P_{s0} = (\frac{0.2941}{Z^{3/2}} + \frac{0.6784}{Z^3})$	(Eq.4)

Tab.1 The incident overpressure versus scaled distance

The peak incident pressure can be converted to peak reflection pressure on the wall normal to the direction of wave propagation by the equation given in [5]

$$P_{r0} = \begin{cases} 2P_{s0} + \frac{6{P_{s0}}^2}{P_{s0} + 0{,}710} & P_{s0} \le 1{,}0 \\ (4\log_{10} P_{s0} + 5{,}5)P_{s0} & P_{s0} > 1{,}0 \end{cases} \quad \text{valid for } \frac{P_{r0}}{P_{s0}} \le 14{,}0 \qquad \text{(Eq.5)}$$

The "peak reflected pressure – scaled distance" relations obtained by substitution of the expressions (1)-(4) for P_{s0} in equation (5) are plotted on a "log-log" plot in Fig. 2 over a shot range including $Z = 0.9062\,m/\sqrt[3]{kg}$. Additionally in Fig. 2 the graph from report [8] is included to draw a comparison. One can see a wide spread of the values predicted by different authors. At the same time the graph from report [8] seems to represent nearly an average curve in the shown region of Z. On the other hand as noted in [4] the equations (1) and (2) for the values $Z < 1.0$ correspond to the conditions of a nuclear explosion. That is the reason why the properties of the shock wave defined in the source [8] has been considered as representative and conservative for the conditions discussing in our paper (detonation of conventional high explosives).

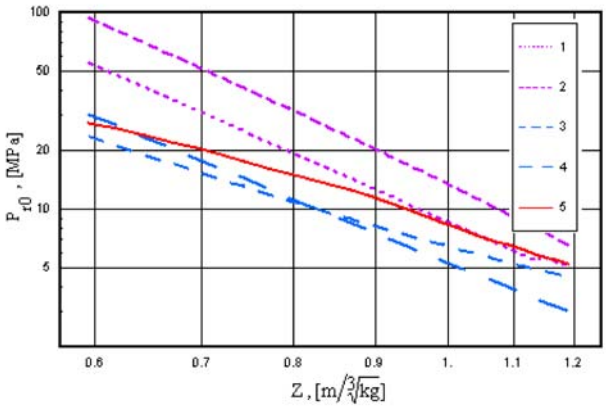

Fig.2 Peak reflected pressure according to (Eq.5) and the relations in Tab. 1: 1-(Eq.1), 2-(Eq.2), 3-(Eq.3), 4-(Eq.4); curve 5- from source [8]

Given the many uncertainties involved in the evaluation of the blast loads, it is recommended [6] that the actual blast effects in the incidental and reflected shock waves may be approximated by equivalent triangular pulses. As mentioned above we additionally consider the blast loads as synchronously acting on all cask surfaces. Then the pressure-time relations can be described as follows:

$$P(t) = \begin{cases} P_{r0}\,(1-\dfrac{t}{t_0}), & \text{front surface} \\ P_{s0}\,(1-\dfrac{t}{t_0}), & \text{side and rear surfaces} \end{cases} \quad \text{with the duration } t_0 = \frac{2\,I_r}{P_{r0}}; \qquad \text{(Eq.6)}$$

where I_r represents the reflected impulse per unit area. The value of I_r can be obtained from a diagram in [8] depending on the scaled distance. Taking into account the safety factor of 1.2 for the "effective charge weight" proposed in [8] we defined finally the parameters for the loading functions (Eq.6) as shown in Tab. 2.

t_0 , [ms]	P_{s0} [MPa]	P_{r0} [MPa]	I_r [Pa×s]
8.5	2.0	12.0	51000

Tab. 2 The pertinent load parameters

3. FE-Analysis of a Transport Cask Subjected to Blast Loading

A few simple estimations may be made on the basis of the parameters defined in Tab. 2. Considering the cask as a free rigid body resting on a smooth surface, we get the maximum velocity of the cask accelerated by the reflection pressure (6) as $\mathrm{v} = \dfrac{I_r \times \pi \times d^2}{4\,M}$. For the spent fuel casks with a mass M varies usually from 80 to 140 metric tons and the diameters of the impact limiters d varies from 2 to 3 m, the upper limit of the velocity after such kind of explosion can be estimated by about 4.5 m/s. This value is much lower than the test velocity of the Type B cask for the 9 m drop onto unyielding target, but comparable with velocity of the cask in case of the 1 m drop onto a punch. Therefore the requirements having to be fulfilled for the approval of the cask are covering the loading of the cask crashing with 4.5 m/s after the explosion.

It is interesting to note that the maximum incident pressure P_{s0} of 2 MPa acting on the side wall of the cask is equal to the static pressure in the 200 m water immersion test which also has to be considered by its approval. This pressure is normally not critical for the robust spent fuel casks. Nevertheless in order to estimate the dynamic effects of the explosion on the side wall the FE analysis was carried out for the model of the whole cask. The cylindrical cask body, the primary and secondary lids and the impact limiters were simulated by means of the isoparametric, three-dimensional, cubic continuum elements with linear interpolation and reduced integration. The bolts connecting the lids and the impact limiters with the cask body were not included in this model. Instead of the bolts appropriate tied conditions were used. For the cask body consisting of ductile cast iron and for the steel lids

an elastic-plastic material law with a v.-Mises yield condition and isotropic hardening was considered. The compound behaviour of the energy absorbing wood material as well as of the sheet metal structure of the impact limiter lining was described by the material model “CRUSHABLE FOAM”.

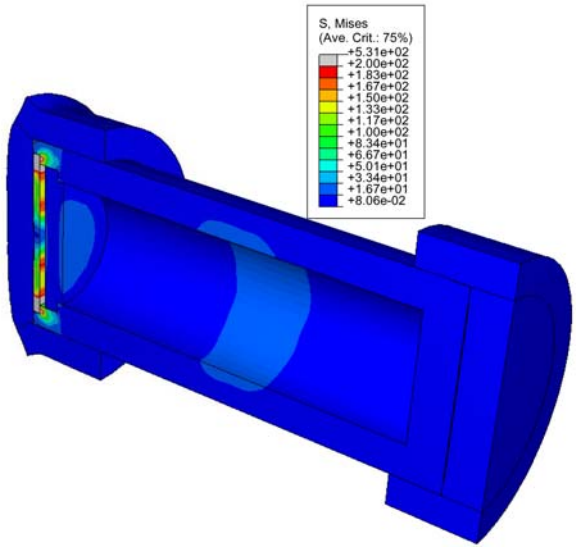

Fig. 3 Example of the stress field in the cask loaded by blast wave (effective stress [MPa])

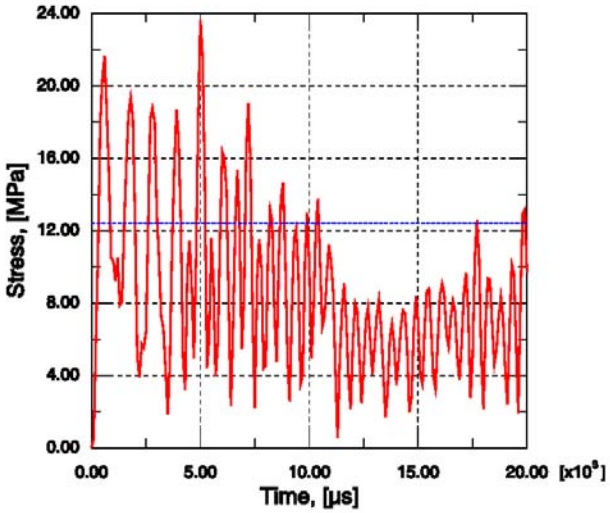

Fig. 4 Effective stress in the cask body

As expected, the lid system is the most loaded part of the cask (Fig. 3). On the contrary the effective stress in the cask body remains quite low and does not exceed the value of 24 MPa. The typical effective stress- time history for the side wall is shown in the Fig. 4. The calculation for the static pressure of 2 MPa showed the maximum effective stress of 12.4 MPa.

In order to examine the stress and deformation behaviour of the lid system more exactly, two detailed FE models of this area were created. The first model (T-Cask) simulates the top part of the cask used only for transport of spent fuel (Fig. 5). The containment system in this case includes only one closure lid with its elastomere gaskets. The

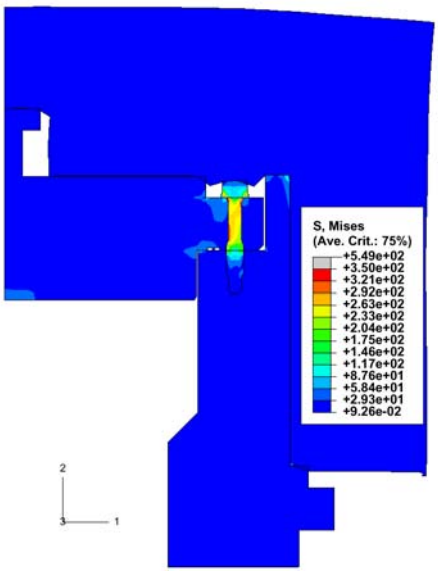

Fig. 5 Stress field in the T-Cask at the end of the blast loading (effective stress [MPa])

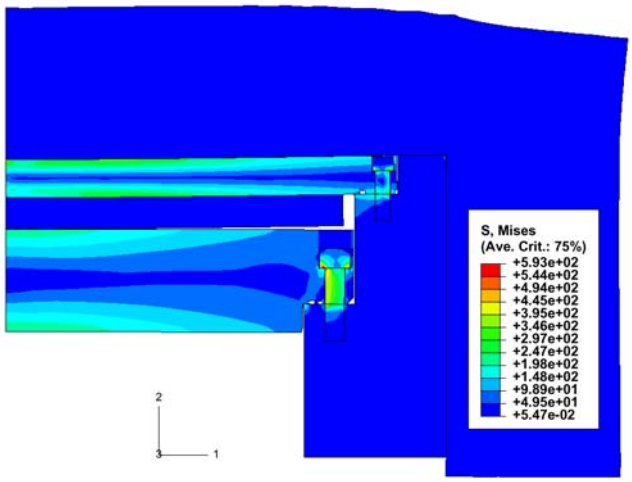

Fig. 6 Stress field in the TS-Cask at the end of the blast loading (effective stress [MPa])

second model (Fig. 6) simulates the double lid system of a transport and storage cask (TS-Cask) with its usually used metallic gaskets.
Both FE models include lids with gasket grooves and lid bolts, the top impact limiter and the top section of the cask body limited in axial direction. The gaskets are not simulated. The FE model of the TS-Cask includes also a moderator plate between the primary and secondary lid. For all parts of a model (except the bolts) axisymmetric elements were used. The geometry of the bolts was smeared to a single plane stress elements submodel. Each plane stress element represents the volumes of all bolts that extend out of the axisymmetric plane. The description of this procedure is presented in [2]. The same material laws as in the FE model considered above were used for the various parts of the construction. The weakness of material in the bolt holes regions of the both lids was taken into account by definition of inhomogeneous material properties for these regions. The nodes on the bottom surface of the cask section were fixed in the axial direction. With a special option of the FE program a pre-tension was applied to the lid bolts and then the cask was loaded with an outer pressure according to (Eq.6).

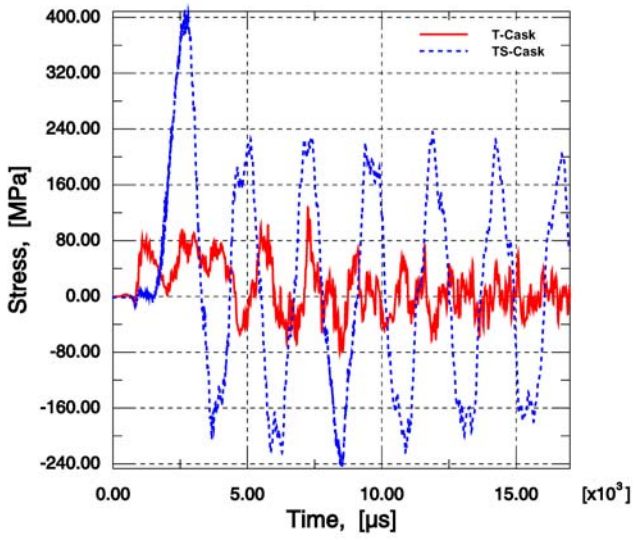

Fig. 7 History of the bending stress in the primary lids

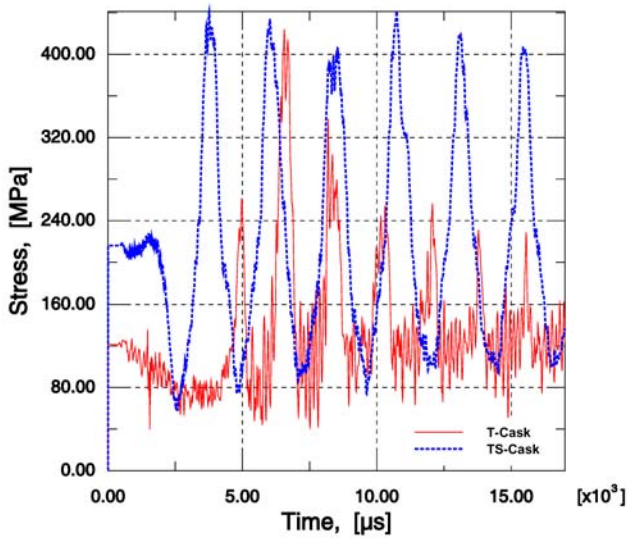

Fig. 8 History of stress in the primary lid bolts

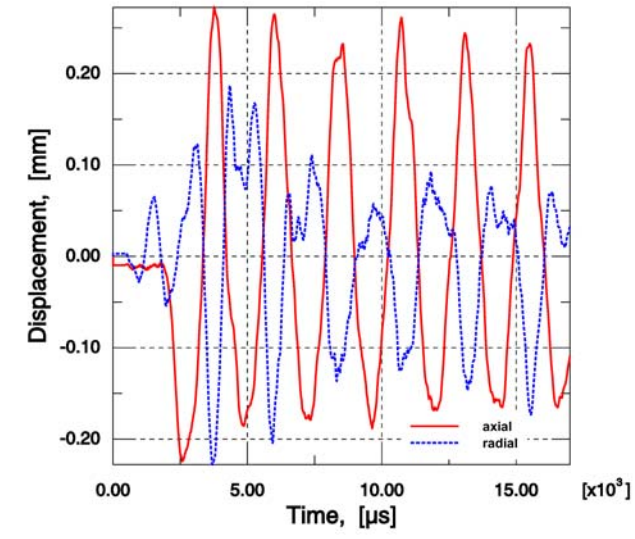

Fig. 9 Sliding (radial) and opening (axial) displacements at the groove of the metallic gasket of the primary lid of the TS-Cask

In Fig. 5 the deformed shape of the lid system of the T-Cask and the stress distribution at the time 8.5 ms after the blast wave impinged onto the construction are presented. Fig. 6 shows the TS-Cask at the same time instant.
The bending stress histories in the primary lids of both casks are compared in Fig. 7. The stress histories in the screws of both primary lids are shown in Fig. 8. The calculations showed the intense oscillations of the primary lids with the maximum bending stress of about 2/3 of the yielding stress of the steel used. The stresses in the screws oscillate about the pre-tension level and remain in the elastic area of the screw material. It can be seen that no loss of the bolt pre-tension occurs. Taking into account the stressing of the primary lid as well as of the primary lid screws a loss of the mechanical integrity can be excluded for both type of casks.

Because a metallic gasket is more sensitive to movements than the elastomere one, the relative displacements between the primary lid and the cask body in the area of the gasket groove were determined for the TS-Cask (Fig. 9). It can be derived from Fig. 7 that the vi-

brations of the primary lid cause the changeable compression of the gasket and additionally its changeable radial displacement. The maximum values of the axial and the radial relative displacements are 0.27 mm and 0.23 mm respectively. From the force-deflection curve and from experiments with Helicoflex metal gaskets [9, 10] it is known that horizontal and vertical displacement as shown in Fig. 9 leads to an increasing of the leakage rate. Because of the fact, that the gasket type used can bear several further compressions and decompressions [9], and that the screws keep their pre-tension, the leak tightness remains well above that limit to ensure an activity release below the IAEA Regulations limit for accident conditions. The conservative values of leakage rate can be assessed by comparison of the calculated relative displacement with test results.

4. Conclusions

The effect of the detonation of 21 t explosives in a distance of 25 m to the cask was considered as a hypothetical representative scenario for the case of an accident of a train containing the spent fuel casks and also wagons with explosives. The conservative estimation of the blast loading onto the casks due to the detonation of explosive was carried out. The response of two types of transport spent fuel casks was analysed by means of FE calculations. Results of the calculations show that the robust transport spent fuel casks preserve their mechanical integrity under explosion conditions.

References

[1] Droste, B. et al.
Impact of an Exploding LPG Rail Tank Car onto a CASTOR Spent Fuel Cask.
RAMTRANS, 10 (1999), No. 4, pp. 231-240

[2] Wieser, G., Qiao, L., Völzke H., Wolff, D. and Droste, B.
Safety Analysis of Casks under Extreme Impact Conditions.
PATRAM 2004, 20-24 Sept. 2004, Berlin, Germany,

[3] ABAQUS Version 6.4
Hibbit, Karlsson & Sorensen Inc.,Pawtucket, Rl., 2003

[4] Henrych, J.
The dynamics of explosion and its use. Amsterdam: Elsevier, 1979.- 560pp

[5] Low, H.Y., Hao, H.
Reliability analysis of reinforced concrete slabs under explosive loading.
Structural Safety, Vol. 23, pp. 157-178 (2001)

[6] Beshara, F.B.A.
Modelling of blast loading on aboveground structures. I. General phenomenology and external blast.
Computer & Structures, Vol. 51, No. 5, pp. 585-596, (1994)

[7] Strehlow, R.A., Baker, W.E.
The characterization and evaluation of accidental explosions.
Progress in Energy and Combustion Science Vol. 2, No. 5, pp. 27-60, (1976)

[8] Structures to resist the effects of accidental explosions.
United States Departments of the Army, Navy and Air Force, TM5-1300 (NAVFAC P-397, AFM 88-22), (1969)

[9] Weise, H.P. et al.
Untersuchung von Dichtsystemen und dichten Umschließungen zum Transport und zur Lagerung radioaktiver Stoffe, Report Forschungsvorhaben ST.-Sch. 943 (Berlin:BAM, 1986)
BMU-Sicherheitsreihe, Reaktorsicherheit und Strahlenschutz, BMU-1989-210

[10] Matsuoka, T. et al.
Verification of Packages Containment System Using Metallic Gasket to Comply with Requirement for both Transport and Storage.
Revised Proc. PATRAM 2001, 3-8 Sept. 2001, Chicago, USA (CD-ROM) INMM, USA (2001)